

**Brazilian Journal of
Chemical Engineering**

**SIMULATION OF SPECIES CONCENTRATION DISTRIBUTION
IN REACTIVE FLOWS WITH UNSTEADY BOUNDARY
CONDITIONS**

Journal:	<i>Brazilian Journal of Chemical Engineering</i>
Manuscript ID	BJCE-2016-0044
Manuscript Type:	Original Article
Date Submitted by the Author:	21-Jan-2016
Complete List of Authors:	DE OLIVEIRA FILHO, ALCESTES; Universidade do Estado do Rio de Janeiro, PPG-EM Mangiavacchi, Norberto; Universidade do Estado do Rio de Janeiro, PPG-EM Pontes, José; Universidade do Estado do Rio de Janeiro, PPG-EM
Keyword:	Finite Element Method, Implicit Finite Differences, Incompressible Reactive Flows, Unsteady Boundary Conditions, Concentration Profile Simulation

SCHOLARONE™
Manuscripts

1
2
3 **SIMULATION OF SPECIES CONCENTRATION**
4
5 **DISTRIBUTION IN REACTIVE FLOWS WITH**
6
7 **UNSTEADY BOUNDARY CONDITIONS**
8
9

10
11
12 A. G. de Oliveira Filho¹, N. Mangiavacchi² and J. Pontes³
13
14

15
16 UERJ – Universidade do Estado do Rio de Janeiro, GESAR
17

18 Rua Fonseca Teles 121, São Cristóvão, 20940-903
19

20 Phone: +(55)(21) 2332-4733, Rio de Janeiro – RJ, Brazil
21

22 Email: ¹ade_oliveira@hotmail.com, ²norberto @uerj.br,
23

24 ³jose.pontes@uerj.br
25

26
27
28
29
30
31
32
33
34
35
36
37
38
39
40
41
42
43
44
45
46
47
48
49
50
51
52
53
54
55
56
57
58
59
60 ¹To whom correspondence should be addressed

1
2
3
4
5
6
7
8
9
10
11
12
13
14
15
16
17
18
19
20
21
22
23
24
25
26
27
28
29
30
31
32
33
34
35
36
37
38
39
40
41
42
43
44
45
46
47
48
49
50
51
52
53
54
55
56
57
58
59
60

Abstract - A numerical model to study chemically reacting species concentration distribution in two-dimensional incompressible flows with unsteady boundary conditions and known velocity profile is presented. The model can be used in transient chemical reactor operation as well as in the study of degradable pollutant concentration in a river. A semi-discrete formulation with Galerkin Finite Element Method and implicit finite differences scheme is employed to solve the governing equation, allowing to calculate the transient concentration distribution along a stream. A new approach to represent the equilibrium condition at the outlet, by the use of the material derivative, is introduced and compared to existing solutions. Results are obtained for various conditions, in order to show features of the code. The model presents itself as a flexible tool, allowing calculations with lateral components of velocities and diffusivities and non-constant rate of reaction.

Keywords — Concentration Profile Simulation, Finite Element Method, Implicit Finite Differences, Incompressible Reactive Flows, Unsteady Boundary Conditions.

INTRODUCTION

The determination of species concentration profiles in incompressible reactive flows presents practical interest to many engineering applications, such as tubular chemical reactors design and operation, concentration evolution prediction of degradable and non-buoyant contaminants in rivers, downstream industrial wastewater or domestic sewage discharge, etc.

While reactants in chemical reactors are subjected to transformation due to chemical or biochemical reactions, pollutants in rivers may also disappear by physical processes, such as volatilization or reactive decay, all of which being accounted for in the transport equation by addition of a reaction term r (van der Perk, 2013):

$$\frac{\partial C}{\partial t} = -\bar{u}_{x_i} \frac{\partial C}{\partial x_i} + D_{x_i} \frac{\partial^2 C}{\partial x_i^2} \pm r \quad (1)$$

After a certain initial time interval, when the mixing processes ~~are~~ ^{IS} completed, species concentration along the flow can be modeled by the use of equation 1. In ideal tube reactors, often treated as plug flow devices, the molecular diffusion and radial/lateral velocities terms may be dropped (Levenspiel, 1999), leading to one-dimensional (1-D) pure advective-reactive model. In other cases, one or both must be taken into account, what asks for two-dimensional (2-D) models. In steady and not very large rivers and channels, it is also

1
2
3 reasonable to assume 1-D convective and diffusive flow,
4 mainly when the controlled length is ten or more times its
5 width (Kachiashvili et al., 2007). In larger watercourses, by its
6 turn, where the river depth is significantly small compared to
7 its width, depth-averaged concentrations assuming vertically
8 well-mixed species could be accounted for (Lee and Seo,
9 2007), making ^{it} possible to apply a 2-D model derived from
10 equation 1.

11
12
13 A number of papers devoted to the advection-dispersion
14 equation, with or without the reaction term, providing both
15 analytical and numerical solution for several cases are found in
16 the literature. O'Loughlin and Bowmer (1975), for instance,
17 applied analytical solutions to equation 1 in 1-D channel flows
18 with decaying species, later extended by Chapman (1979) to
19 non-uniform steady rivers, both considering instantaneous or
20 continuous inlet and prescribed outlet concentrations.
21
22 Comparison with the results obtained in the experimental works
23 of Vilhena and Leal (1981) for non-reacting pollutants shows
24 good agreement between both. Czernuszenko (1987), also
25 working with dispersion of conservative species, proposed a
26 numerical solution to the 2-D advection-dispersion equation,
27 bounded by natural boundary conditions (NBC), using a
28 conditionally stable finite differences (FD) scheme.
29 Kaschiashvili et al. (2007) provided a consistent model for river
30 reactive flow problems in one, two and three dimensions and
31
32
33
34
35
36
37
38
39
40
41
42
43
44
45
46
47
48
49
50
51
52
53
54
55
56
57
58
59
60

| PE

OL
CONJ IS A
CASE OF A MULTIDIMEN-
SIONAL FLOW PROBLEM

1
2 used dimension-splitting FD numerical schemes, with unsteady
3 upstream boundary condition (BC) and a NBC downstream.
4
5 But, due to the equilibrium condition at the outlet, consisting of
6 a constant spatial concentration gradient, this BC no longer
7 applied and has been modified, sometimes, with the
8 introduction of an additional parameter in order to better
9 reproduce experimental data. Lee and Seo (2007) used a 2-D
10 Finite Element Model (FEM), based on the Streamline-Upwind
11 Petrov-Galerkin Method together with a Crank-Nicholson FD
12 scheme for the time derivative, as in this paper, but restricted to
13 rivers where the process is diffusion dominated and the
14 downstream BC was a prescribed diffusion flux.

15 Works modeling fluid dynamics by FEM, in chemical
16 reactors, are not commonly found in the literature. Ranade's
17 (2002) book on reactors computational fluid modeling employs
18 the finite volume method, in the examples and applications
19 presented. Sometimes, commercial packages using the FEM on
20 their built-in routines are employed for the study of chemical
21 reactors models performance (Galante, 2012; Mushtaq, 2014).
22
23 However, in addition to being proprietary, these routines often
24 focus simulations of chemical reaction media, rather than flow
25 dynamics. Yet, it is possible to verify, in the works by
26 Skrzypacz and Tobiska (2005) and Skrzypacz (2010), a FEM
27 scheme to solve a simple 1-D reactive flow in packed bed
28 reactors. Even though in these latter two studies the transport
29

equations are steady, the BCs are of the Dirichlet type and the reaction term is not explicitly solved, the validity of using FEM in chemical reactors flow modeling is pointed out.

Thus, additional motivation exists for the study of concentration fields developed in two dimensional incompressible flows using the FEM, to simulate problems modeled by equation 1 and subjected to unsteady BCs. This is the case of tubular chemical reactors operating under variable inlet feed, due to diversified production, or when pollutant with variable species concentration spills in rivers and channels. Special attention must be given to the form of the outlet BC. When the input concentration is unsteady, the exit concentration or the species flux is an unknown and assuming prescribed values at the outlet is not realistic. Up to now, this is being solved either by suppressing the outlet concentration gradients, what may be physically unrealistic (Ziskind et al., 2011) or by adopting Robin type BCs (Golz and Dorroh, 2001). Our proposal is to use an outlet BC in the form of a material derivative, directly representing the concentration gradient or the species flux time dependence.

Some publications containing mostly 1-D analytical solutions of the convection-diffusion-reaction equation subjected to time varying BCs, like van Genuchten and Alves (1982), Logan and Zlotnik (1995), Logan (1996), Aral and Liao (1996) and Golz and Dorroh (2001) may be cited. But to the authors'

knowledge, no analytical solution considering a material derivative as the outlet BC was yet constructed. So, a computer code prototype was developed in MATLAB, in order to search for a numerical solution.

A semi-discrete formulation with a Galerkin FEM (GFEM) and implicit FD scheme is then used to solve a simple 2-D convection-diffusion-reaction equation (equation 1). The inlet, or upstream, unsteady BC behavior is assumed either as time periodic, or as pulse functions, providing a variable condition. At the outlet, or downstream, to better represent the equilibrium condition among diffusion, advection and reaction in unsteady conditions, the outlet flux is evaluated by the species concentration material derivative.

MATHEMATICAL FORMULATION

Considering the objectives of the present study, of addressing isothermal reactive flows, an average hydrodynamic field is assumed, so turbulence models are not introduced in the evolution equations. We emphasize that averaging the concentration field along one of the three directions, in order to construct 2-D models, requires that reactants or pollutants be mixed at a much faster rate than the reaction rate, as in the microfluid idealization (Levenspiel, 1999).

The reaction term in equation 1 may considerably vary, depending on the process. For simplicity, it was decided to

analyze only a first order reaction model. The transport equation then becomes:

$$\frac{\partial C}{\partial t} = -\bar{u}_{x_i} \frac{\partial C}{\partial x_i} + D_{x_i} \frac{\partial^2 C}{\partial x_i^2} + kC \quad (2)$$

with initial condition given by:

$$C(x_i, 0) = 0 \quad (3)$$

BCs used at the inlet or upstream are prescribed in one of the two forms below:

$$\left. \begin{array}{l} C_{inj}(0, y, t) = 0, \quad 0 \leq t < n\tau \\ C_{inj}(0, y, t) = C_{inj}, \quad t = n\tau \end{array} \right\} \quad (4)$$

in order to represent a short injection at times $n\tau$, or to represent a periodic injection, we assume :

$$C_{inj}(0, y, t) = C_i (1 + \cos m\pi t) \quad (5)$$

where C_i is the amplitude of the species concentration at the inlet. In equations 4-5, the y coordinate is applicable to 2-D flows and may represent injection in part or along all its length.

As already mentioned, analytical solutions for this kind of problem exist and will be used in order to validate numerical results. These solutions assume either prescribed or Neumann's outlet BCs mostly at semi-infinite domains. Moreover, even the solutions for finite domains that accept one or other of those BC are subjected to criticism (Ziskind, 2011).

Equation 2 is solved by a FEM scheme, with a Galerkin formulation. So a weighted residual statement of that equation reads:

$$\int_{\Omega} \left(\frac{\partial C}{\partial t} + \bar{u}_i x_i \frac{\partial C}{\partial x_i} - D x_i \frac{\partial^2 C}{\partial x_i^2} - kC \right) w d\Omega = 0 \quad (6)$$

By applying the divergence theorem to the third term of the above equation, and substituting the result in equation 6, the following weak form is obtained:

$$\int_{\Omega} \left(w \frac{\partial C}{\partial t} + w \bar{u}_i x_i \frac{\partial C}{\partial x_i} + D x_i \frac{\partial w}{\partial x_i} \frac{\partial C}{\partial x_i} - k w C \right) d\Omega = \int_{\Gamma} w D \left(n_i \frac{\partial C}{\partial x_i} \right) d\Gamma \quad (7)$$

where $D = \sqrt{D_x^2 + D_y^2}$ and $\Gamma = \Gamma_{in} \cup \Gamma_1 \cup \Gamma_2 \cup \Gamma_{out}$

Γ_1 and Γ_2 represent lateral surfaces and the related fluxes are zero. Γ_{in} , by its turn, represents the inlet boundary, subjected to specified, but time-dependent, BCs, as given by equations 4-5. In this case, the weight functions are zero for Γ_{in} , implying that the surface integral is only evaluated along Γ_{out} .

By looking again at the r.h.s. of equation 7, it can be verified that the weak formulation boundary term represents the Fick's Law. Yu and Singh (1995) sustain that this formulation should be only applied to situations where there are exclusively diffusion fluxes at the outlet boundary. But in the problems under consideration, it is plausible that advection might effectively occur at the outlet, and said term no longer represents the total exiting flux.

However, there are cases where gradients normal to the outlet surface are zero, bringing the formulation back onto consistency, even in presence of convection because it eliminates that surface integral:

$$\frac{\partial C}{\partial x_i} \Big|_{\Gamma_{out}} = 0 \Rightarrow \int_{\Gamma_{out}} w D \left(n_i \cdot \frac{\partial C}{\partial x_i} \right) d\Gamma_{out} = 0 \quad (8)$$

We must have in mind that for a developed profile, it also implies, by accounting for equation 2, in:

$$\frac{\partial C(x_i, t)}{\partial t} \Big|_{\Gamma_{out}} = kC(x_i, t) \rightarrow 0 \quad (9)$$

We emphasize that this condition does not hold when the gradients at the outlet are not zero. By the way, it is well known that flow problems involving the transport of chemical species with NBC fail to satisfy the conservation law for species concentrations within the domain (Golz and Dorroh, 2001). In particular, prescribed constant outlet fluxes (EBCs) also do not lead to correct description of time dependent problems.

So, for the sake of generality and considering that in rivers, flow channels and also, in tubular reactors where the dispersion is mainly due to vertical and transverse velocity gradients, while molecular and turbulent diffusions are generally negligible (Launay et al., 2015), another outlet BC must be assumed. So, adding the advection term to equation 9, one has:

$$\left(\frac{\partial C(x_i, t)}{\partial t} + \bar{u}_{x_i} \cdot \frac{\partial C(x_i, t)}{\partial x_i} \right) \Big|_{\Gamma_{out}} = kC(x_i, t) \Big|_{\Gamma_{out}} \quad (10)$$

Equation 10 is in fact a nonhomogeneous material derivative that automatically evaluates the spatial gradients at the outlet boundary. Combining equations 7 and 10, it is possible to write:

$$\int_{\Omega} \left(w \frac{\partial C}{\partial t} + w \bar{u}_x \cdot \frac{\partial C}{\partial x_i} + D_{x_i} \frac{\partial w}{\partial x_i} \cdot \frac{\partial C}{\partial x_i} - k w C \right) d\Omega = \int_{\Gamma_{out}} w \frac{D}{U} \left(k C - \frac{\partial C}{\partial t} \right) d\Gamma_{out} \quad (11)$$

where $U = \sqrt{\bar{u}_x^2 + \bar{u}_y^2}$. Then, equation 11 is the one to be numerically implemented by GFEM, in order to obtain the species concentration profiles.

The numerical procedure may be tested by comparing the results with preexisting analytical solutions. In the simplest case of 1-D flow, analytical solutions for continuous and instantaneous mass injection, are, respectively (O'Loughlin and Bowmer, 1975; Chapman, 1979):

$$\frac{C(x,t)}{C_{inj}} = \frac{1}{2} \exp\left(\frac{-kx}{\bar{u}_x}\right) \operatorname{erfc}\left[\frac{x - \bar{u}_x t (1 + H_x)}{\sqrt{4 D_x t}}\right] \quad (12)$$

and:

$$C(x,t) = \frac{M_{inj}}{\sqrt{4\pi D_x t}} \exp\left[-kt - \frac{(x - \bar{u}_x t)^2}{4 D_x t}\right] \quad (13)$$

where $H_x = \frac{2kD_x}{\bar{u}_x^2}$ and M_{inj} is the total mass injected per unit area. And for a 2-D case with short pulse injection where there is a transversal diffusion D_y and zero lateral component of velocity (Vilhena and Sefidvash, 1985):

$$C(x,y,t) = \frac{M_{inj}}{4\pi t \sqrt{D_x D_y}} \exp\left[-kt - \frac{(x - \bar{u}_x t)^2}{4 D_x t} - \frac{y^2}{4 D_y t}\right] \quad (14)$$

When the inlet BC is given by equation 5, an onedimensional analytical solution may be obtained. By following the work of

Logan and Zlotnik (1996), it is possible to establish that equation 2 clearly admits a solution of the form:

$$C(x,t) = e^{\hat{\alpha}x + \hat{\beta}t} \quad (15)$$

where $\hat{\alpha}$ and $\hat{\beta}$ are complex valued, thus:

$$\hat{\alpha} = \alpha_R + i\alpha_I \quad \text{and} \quad \hat{\beta} = \beta_R + i\beta_I \quad (16)$$

Then, substituting equations 15-16 in 1-D equation 2 type, one obtains:

$$\hat{\beta} = k - \bar{u}_x \hat{\alpha} + D_x \hat{\alpha}^2 \quad (17)$$

Once the periodic BC forces the inlet concentration at a fixed value, $\beta_R = 0$ and the solution may be expressed as:

$$C(x,t) = R[e^{(\alpha_R + i\alpha_I)x + i\beta_I t}] \quad (18)$$

where R means the real part of equation 18 and:

$$\alpha_I = \pm \sqrt{\alpha_R^2 - \frac{\bar{u}_x}{D_x} \alpha_R - \frac{k}{\bar{u}_x}} \quad \text{and} \quad \beta_I = \pm \sqrt{\alpha_R^2 - \frac{\bar{u}_x}{D_x} \alpha_R - \frac{k}{\bar{u}_x}} (2D\alpha_R - \bar{u}_x) \quad (19)$$

Also, considering that the concentration at $x = 0$ cannot take negative values, it is necessary to add a constant forcing, such that this restriction is satisfied, and equation 18 becomes:

$$C(x,t) = C_o + R[e^{(\alpha_R + i\alpha_I)x + i\beta_I t}] \quad (20)$$

For this constant forcing, obviously $\beta_R = \beta_I = 0$ and therefore, with the use of equation 19:

$$\hat{\alpha}_o = -\frac{\bar{u}_x}{2D_x} \pm \sqrt{\frac{\bar{u}_x^2}{4D_x} - \frac{k}{D_x}} \quad (21)$$

what implies in:

$$C_o = R[e^{(\hat{\alpha}_o)x}] \quad (22)$$

Thus, given k , \bar{u}_x and D_x , as well as an arbitrary α_R , the analytical solution may be constructed, employing equations 19-22.

NUMERICAL PROCEDURE

By using the Galerkin formulation, the concentration profile is approximated by:

$$C_{app}(x_i, t) = \sum_{j=1}^{NN} C_j(t) S_j(x_i) \quad (23)$$

Substituting this approximation into the weak form given by equation 11, where, according to the GFEM, the weight functions are the same as the shape functions (Zienkiewicz and Taylor, 2000), one has:

$$\begin{aligned} & \sum_{j=1}^{NN} \left[\int_{\Omega} S_i S_j d\Omega + \frac{D}{U} \int_{\Gamma_{out}} S_i S_j d\Gamma_{out} \right] \frac{dC_j}{dt} + \int_{\Omega} S_i \left(\bar{u}_x \frac{\partial S_j}{\partial x} + \bar{u}_y \frac{\partial S_j}{\partial y} \right) + \left(D_x \frac{\partial S_i}{\partial x} \frac{\partial S_j}{\partial x} + \right. \\ & \left. + D_y \frac{\partial S_i}{\partial y} \frac{\partial S_j}{\partial y} \right) d\Omega C_j - k \left(\int_{\Omega} S_i S_j d\Omega + \frac{D}{U} \int_{\Gamma_{out}} S_i S_j d\Gamma_{out} \right) C_j = 0 \end{aligned} \quad (24)$$

where the boundary integral was approximated through:

$$\int_{\Gamma_{out}} S_i (D \vec{n} \cdot \nabla C) d\Gamma_{out} = \sum_{j=1}^{NN} \left[\frac{D}{U} \left(\int_{\Gamma_{out}} S_i S_j d\Gamma_{out} \right) k C_j - \frac{dC_j}{dt} \right] \quad (25)$$

Equation 24 encompasses a stiffness matrix and a modified mass matrix which is related to the concentration time derivative and the reaction term. It can be put under matrix form as:

$$[M_1] \left\{ \dot{C} \right\} + [K] \{C\} - k[M_1] \{C\} = 0 \quad (26)$$

where, M_1 and K are, respectively, the modified mass and stiffness matrices.

A numerical scheme, using the Crank-Nicholson Method (Lewis et al., 2005), reads:

$$\{C_{t+1}\} = \left([M_1] + \frac{\Delta t}{2} (K - k[M_1]) \right)^{-1} \left([M_1] - \frac{\Delta t}{2} (K - k[M_1]) \right) C_t \quad (27)$$

It must be observed that it is also possible to look for another solution without modifying the original mass matrix, as suggested above. In this case, the use of the Crank-Nicholson scheme on the original form of that equation implies in:

$$\{C_{t+1}\} = \left([M] + \frac{\Delta t}{2} [K_1] \right)^{-1} \left[\left([M] - \frac{\Delta t}{2} [K_1] \right) C_t + \frac{\Delta t}{2} (\{B\}_t + \{B\}_{t+1}) \right] \quad (28)$$

where $[M]$ is $\sum_{j=1}^{NN} \int_{\Omega} S_i S_j d\Omega$ and $[K_1]$ is a modified stiffness

matrix, now including the decay term, last on the left term of equation 11, or:

$$\sum_{j=1}^{NN} \left\{ \int_{\Omega} S_i \left(\bar{u}_x \frac{\partial S_j}{\partial x} + \bar{u}_y \frac{\partial S_j}{\partial y} \right) + \left(D_x \frac{\partial S_i}{\partial x} \frac{\partial S_j}{\partial x} + \right. \right.$$

1
2
3
4
5
6
7
8
9
10
11
12
13
14
15
16
17
18
19
20
21
22
23
24
25
26
27
28
29
30
31
32
33
34
35
36
37
38
39
40
41
42
43
44
45
46
47
48
49
50
51
52
53
54
55
56
57
58
59
60

$$\left. + D_y \frac{\partial S_i}{\partial y} \frac{\partial S_j}{\partial y} - k S_i S_j \right) \right] d\Omega C_j \} \quad (29)$$

In this case, the boundary vectors must be evaluated using equation 25. Being dependent on the concentration and its time derivative in past and present time steps, these vectors must be continuously updated, making the numerical scheme for solving equation 27 simpler than the one required for solving equation 28. Thus, we opted for the first scheme.

The code was implemented in MATLAB, taking advantage of its matrix calculation resources. The integrals in equation 24 were evaluated by the Gauss Quadrature (GQ). The solution domain was discretized in regular triangular or quadrangular element meshes by routines within the program, depending on the case run. The program is also capable of performing GQ calculations in diversified number of interval points. Linear shape functions were used throughout this work, so precision of the scheme was controlled by properly refining the mesh.

It is well known that simple GFEM experiences numerical oscillations and instabilities in problems where advection is important, what points to the adoption of more elaborated FEM schemes. But for programming simplicity, once the role of the unsteady BC together with the outlet BC represented by a material derivative were the main aspects to be investigated, this method was employed with restrictions. Aware that some of the major factors causing these issues are improper choice

of a time step size and also of element size and shape (Yu and Singh, 1995), we adopted, as a basis for the time step and element size control, respectively, (Chapra and Canale, 2010):

$$\Delta t_i \leq \frac{(\Delta x_i)^2}{2D_{x_i} + k(\Delta x_i)^2} \quad \text{and} \quad \Delta x_i \leq \frac{2D_{x_i}}{\bar{u}_i} \quad (30)$$

RESULTS AND DISCUSSION

Preliminary Tests

A more detailed look at the analytical solutions presented by equations 12-14 reveals that, actually, the upstream BCs are not time independent, as it may appear to be in a first glimpse. Assuming unitary injection concentration, the analytical solutions result in the plots of Figure 1. As it can be verified, within the stream limits, these BCs show different unsteady profiles characterized by the inlet concentration correction due to particular advective and diffusion effects.

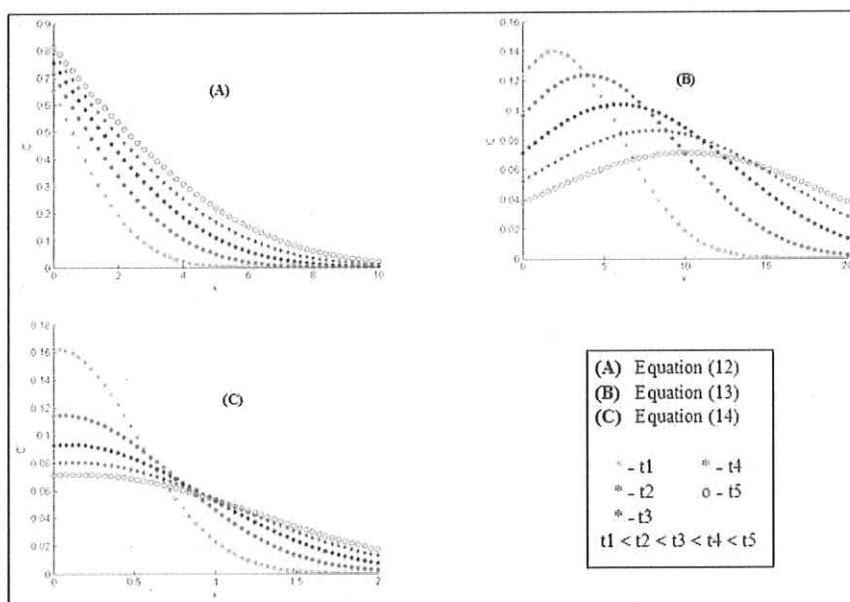


Figure 1. 1-D Plot of Analytical Solutions, Equations 12-14.

(Pe = 5.0, Da = 2.0; Graph C corresponds to centerline injection)

It is well known that the solution form for the concentration profile is (Vilhena and Sefidvash, 1985):

$$C(x,t) = C_o(x,t) \exp(-kt) \quad (31)$$

where C_o is the corrected species concentration to initial time. So, in order to check the code results, the inlet BCs to be applied at $x=0$ will carry on the initial shape of the defined concentration, as suggested by Yu and Li (1998).

Then:

a) for equation 12:

$$C_o(0,t) = \frac{C_{inj}}{2} \left\{ erfc \left[\frac{-\bar{u}_x t (1 + H_x)}{\sqrt{4 D_x t}} \right] \right\} \quad (32)$$

b) for equation 13:

$$C_0(0,t) = \frac{M_{inj}}{\sqrt{4\pi D_x t}} \exp\left[-kt - \frac{(-\bar{u}_x t)^2}{4D_x t}\right] \quad (33)$$

and:

c) for equation 14:

$$C_0(0,y,t) = \frac{M_{inj}}{4\pi t \sqrt{D_x D_y}} \exp\left[-kt - \frac{(-\bar{u}_x t)^2}{4D_x t} - \frac{y^2}{4D_y t}\right] \quad (34)$$

Having that in mind, one can apply equations 32-34 to the MATLAB code and compare the results with the analytical solutions for constant and pulse injection cases.

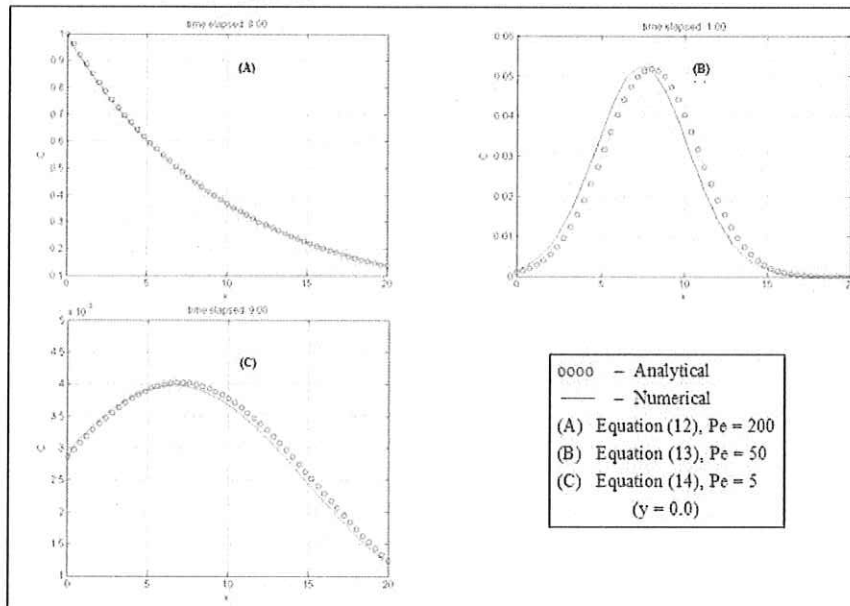


Figure 2. 1-D Analytical and Numerical Solution of Equations 12-14 Cases.

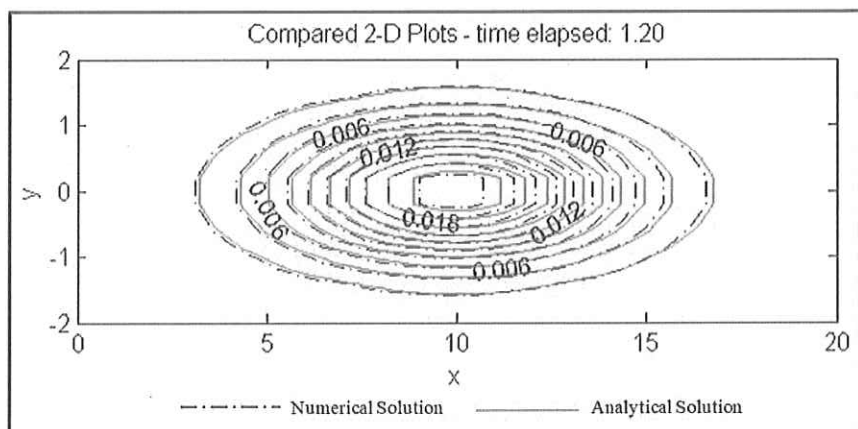


Figure 3. 2-D Analytical and Numerical Solution of Equation 14 Case.

(1250 Elements Mesh; GQ 9 points; Pe = 50)

Conditions for Pe = 200: $\bar{u}_x = 10$, $D_x = 1.0$ and $k = 1.0$; for Pe = 50: $\bar{u}_x = 10$, $D_x = 4.0$ and $k = 1.0$ and for Pe = 5.0: $\bar{u}_x = 1$, $D_x = 4.0$ and $k = 0.1$, resulting in the same Damköhler Number (Da = 2.0) for all cases. For the tests with equation 14, which admits a lateral component of diffusion, D_y was set equal to 0.2 and its 1-D plot (graph C of Figure 2) represents the centerline concentration profile ($y = 0.0$)

The numerical solution of equation 2, for the periodic inlet BC (equation 5), may be compared with the 1-D analytical solution constructed from equations 19-22 through a plot extracted from the centerline concentration profile. Figure 4 shows the outcome for Pe = 100, where $\bar{u}_x = 5.0$, $D_x = 1.0$ and $k = 0.1$, implying in Da = 0.4.

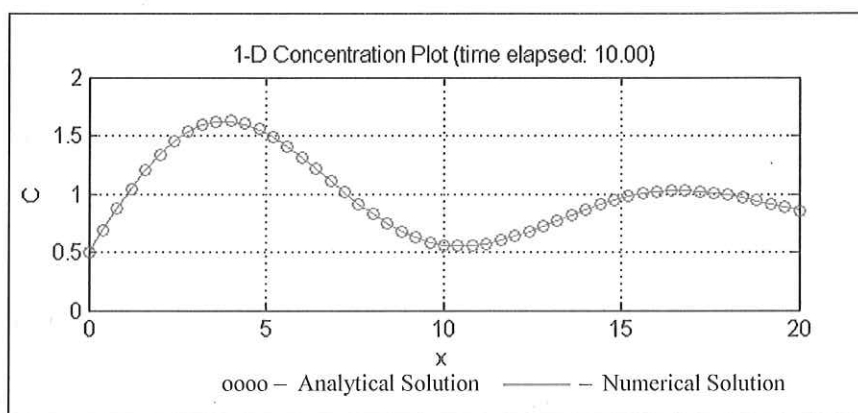


Figure 4. 1-D Analytical and Numerical Solutions of Equation 2 with periodic inlet BC.

(1250 Elements Mesh; GQ 9 points; Pe = 50).

In order to obtain the plots of Figures 2 to 4, we run the code and then compared the results with the analytical solution correspondent to the time run. Numerical calculation was performed, respecting the stability restrictions posed by equations 30. The plots show good agreement between analytical and numerical solutions even for high Péclet Numbers.

It is possible to observe a better agreement for the continuous injection case (equation 12), while the plots in graphs B and C of Figure 2, corresponding to equations 13 and 14, and in Figure 3, related exclusively to equation 14, show that the numerical curves are somewhat delayed compared to the exact solutions. This delay results from the fact that the discrete time integration cannot completely follow the instant moment of mass release (Lee and Seo, 2010).

Comparing Analytical and Numerical Solutions

Figure 5 shows some differences between numerical solutions of equation 2 when a time periodic inlet concentration is imposed. Profiles obtained when the adopted outlet condition is either EBC or NBC, compared to those obtained by the adoption of the MDBC, concentrate larger differences around the exit.

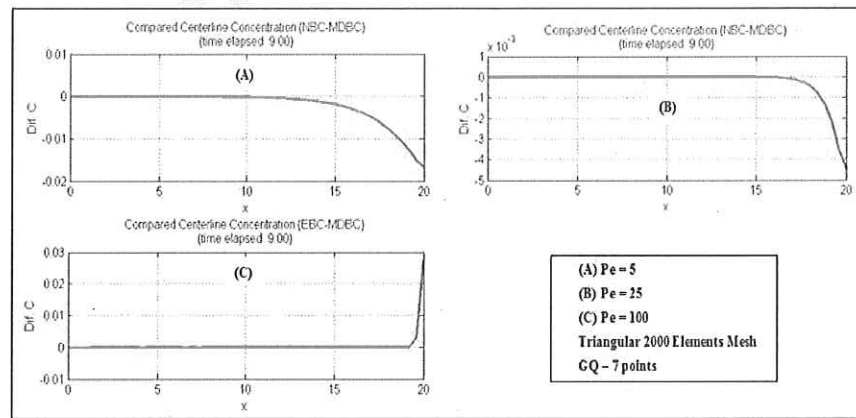


Figure 5. Centerline Concentration Profile Differences – Numerical Solutions.

(Inlet BC: Equation 5; Outlet EBC = 0.5; Outlet NBC: Equation 8; Outlet MDBC: Equation 10).

Conditions are, for $Pe = 5$: $\bar{u}_x = 1.0$, $D_x = 4.0$, and $k = 0.1$; for $Pe = 25$: $\bar{u}_x = 5.0$, $D_x = 4.0$, and $k = 0.1$; and for $Pe = 100$: $\bar{u}_x = 5.0$, $D_x = 1.0$, and $k = 0.1$.

In order to check the validity of the above proposition, we numerically evaluated concentrations 1-D profiles for various flow and reaction parameters. The results were compared to the

analytical solution and analyzed by the Root-Mean-Square Deviation (RMSD), or:

$$\text{RMSD} = \sqrt{\frac{\sum_{i=1}^m (C_i - C_i^a)^2}{m}} \quad (35)$$

where C_i^a is the analytical solution at node i for a given total number of nodes m at the exit region.

Table 1. RMSD between 1-D Analytical and Numerical Solutions.

Pe = 100		RMSD			
Δx	Δt	Da	An. - EBC	An. - NBC	An. - MDBC
0.2	0.02	0.1	0.8193	0.0315	0.0226
		1.0	0.2640	0.1839	0.1744
		2.0	0.0745	0.0044	0.0022
Pe = 50		RMSD			
0.2	0.005	0.1	0.8628	0.0098	0.0041
	0.05	1.0	0.4982	0.0106	0.0032
		2.0	0.1312	0.0809	0.0798
Pe = 25		RMSD			
0.2	0.02	0.1	0.8846	0.0777	0.0537
0.4	0.01	1.0	0.4010	0.0676	0.0679
0.2	0.02	2.0	0.1476	0.0387	0.0259
Pe = 5		RMSD			
0.2	0.05	0.1	0.6155	0.0275	0.0191
	0.2	1.0	0.5672	0.0071	0.0072
	0.1	2.0	0.0880	0.0178	0.0034

(Inlet BC: Equation 5; Outlet EBC = 0.0; Outlet NBC: Equation 8; Outlet MDBC: Equation 10).

We observe that the numerical solutions with outlet EBC provide the poorest approximations in all Péclet and Damköhler

1
2
3
4
5
6
7
8
9
10
11
12
13
14
15
16
17
18
19
20
21
22
23
24
25
26
27
28
29
30
31
32
33
34
35
36
37
38
39
40
41
42
43
44
45
46
47
48
49
50
51
52
53
54
55
56
57
58
59
60

Numbers considered and that MDBC solutions result in better approximations than NBC in almost all cases.

Small Péclet and Damköhler numbers result in very small concentration gradients at the outlet. In this condition, as coarser meshes are adopted, the best results were sometimes obtained by assuming NBC. However, the use of MDBC along with sufficiently fine meshes or refined time steps lead to better matching with the analytical solution than assuming NBC.

2-D Simulation Results

Having in mind the satisfactory results obtained in the tests, we further used the code to investigate the behavior of 2-D systems. Velocities and diffusion constants were chosen as close as possible to real configurations.

For instance, Figure 6 shows the results of 2-D and 1-D simulations under conditions such that the inlet BC is the periodic concentration oscillation given by equation 5, lateral components of velocity and diffusivity are ten times smaller than the longitudinal components ($\bar{u}_x = 5.0$, $\bar{u}_y = 0.5$, $D_x = 1.0$, $D_y = 0.1$ and $k = 0.1$), implying in $Pe = 100$ and $Da = 0.4$.

In this case, convective transport plays a major role overcoming diffusion transport and reaction decay and implies in predicted oscillatory values for the concentration along all the domain.

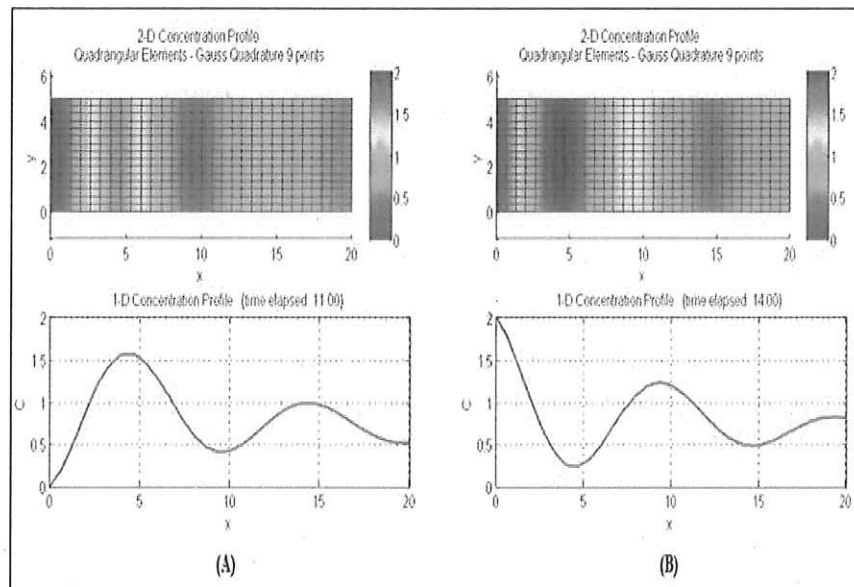


Figure 6. Concentration Profile for Decaying Species.

(900 Elements Mesh - Inlet BC: Equation 5; Outlet BC: Equation 10)

Figure 7 shows the outlet concentrations for $\text{Pe} = 10$ and $\text{Da} = 0.4$ ($\bar{u}_x = 0.5$, $\bar{u}_y = 0.05$, $D_x = 1.0$, $D_y = 0.1$, $k = 0.01$), subjected to the same BCs, implying a more important play for diffusive transport. In addition, smaller flow rates allow the chemical reaction to further evolve as the convective transport takes place. Following, the oscillatory behavior of the inlet concentration is damped before reaching the domain outlet and the solution approaches the typical shape of pure diffusive transport problems subjected to oscillatory BC, known as *periodic steady-state* (Bird et al, 2002).

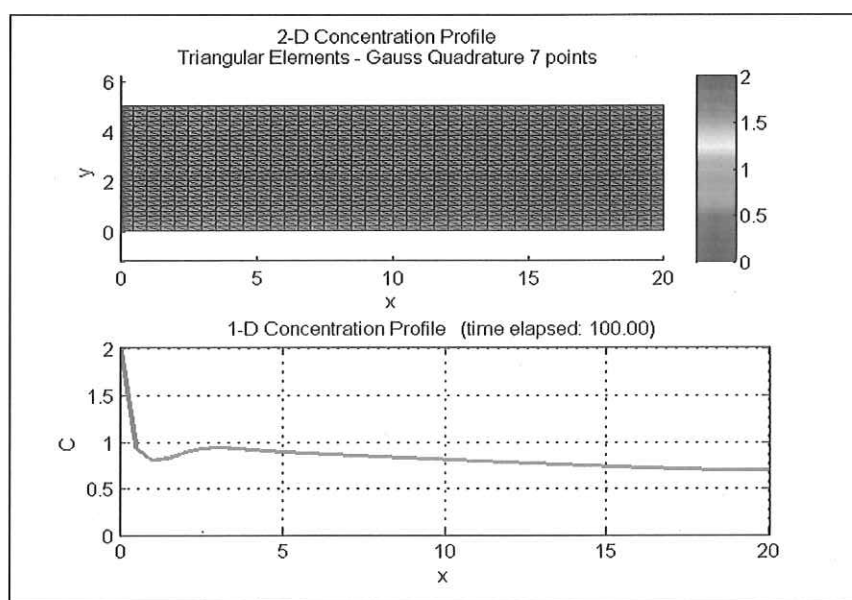


Figure 7. Concentration Profile for Decaying Species.

(2000 Elements Mesh - Inlet BC: Equation 5; Outlet BC: Equation 10)

When equations 5 are applied as the inlet BC, resulting in the injection of time dependent concentrations, the code shows the concentration profiles approaching the oscillatory profile as the interval time between each injection becomes shorter (part A of Figure 8), or the pulse injection profile (part B of Figure 8), in a Gaussian shape, as it becomes larger.

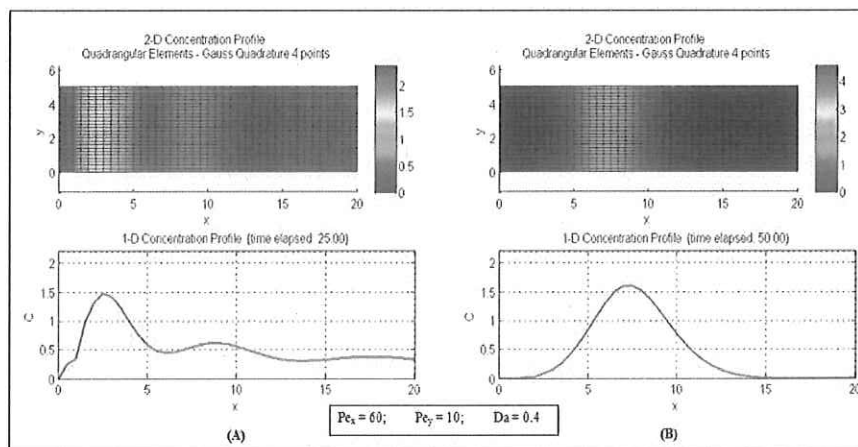


Figure 8. Concentration Profile for Decaying Species.

(1000 Elements Mesh - Inlet BC: Equation 4; Outlet BC: Equation 10)

The code is able to simulate 2-D configurations, including flow predictions when the velocities profiles are steady but dependent on the spatial coordinates such that $\bar{u}_x = \bar{u}_x(y)$ and $\bar{u}_y = \bar{u}_y(x)$. For example, if a steady parabolic profile is considered for the longitudinal velocity (equation 36), for the same other parameters as those of Figure 4, Figure 9 is obtained:

$$\bar{u}_x = 5.0y - y^2 \quad (36)$$

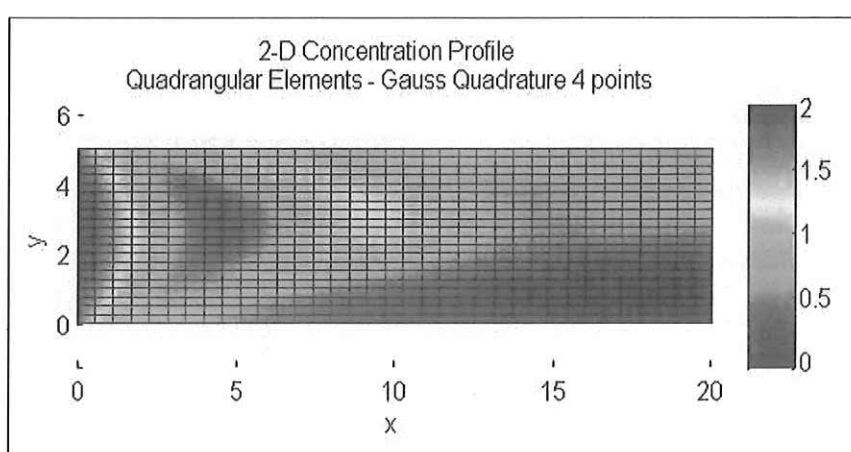


Figure 9. Concentration Profile for Decaying Species – Parabolic Longitudinal Velocity.

(700 Elements Mesh - Inlet BC: Equation 5; Outlet BC: Equation 10)

Figure 9 depicts the evolution of the species cloud deformed due to the existence of lateral components of velocity and diffusion. But the mass injection is set in all the inlet cross section area, what may be most related to chemical reactors cases or small channels. Anyway, it is possible to simulate point source injections, what would be more likely to happen in rivers, by modification of the inlet BC, making it dependent on y , as follows.

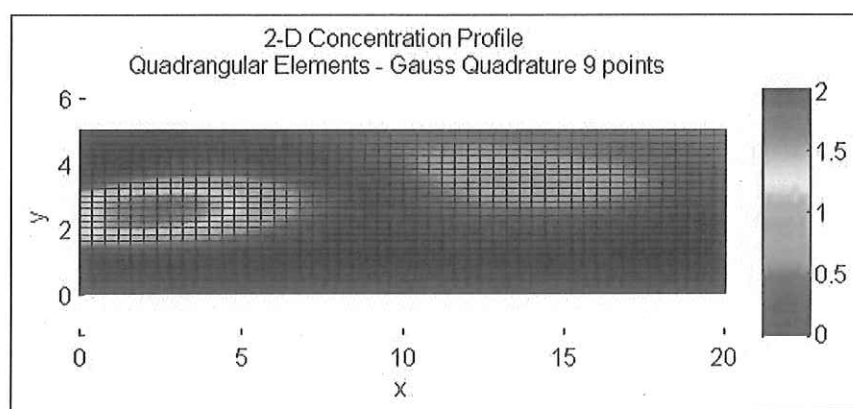


Figure 10. Concentration Profile for Decaying Species – Left centerline injection.

(1250 Elements Mesh - Inlet BC: Equation 5; Outlet BC: Equation 10)

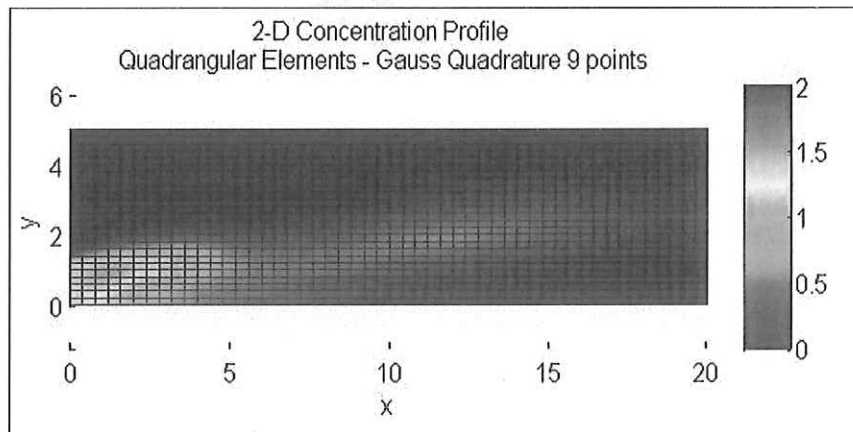


Figure 11. Concentration Profile for Decaying Species – Bottom left injection.

(1250 Elements Mesh - Inlet BC: Equation 5; Outlet BC: Equation 10)

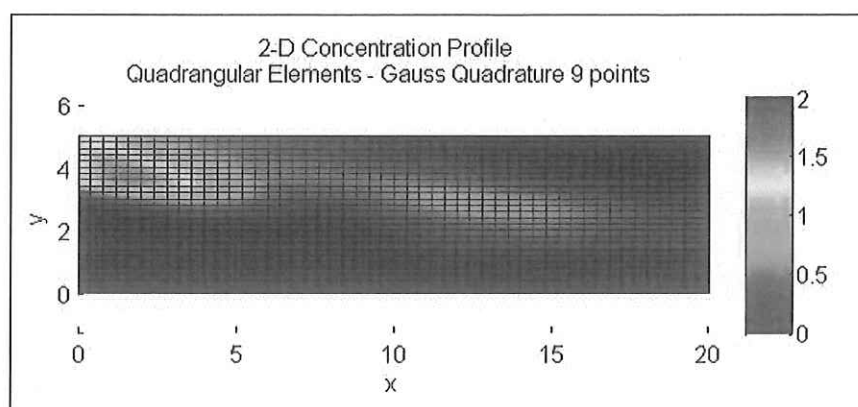


Figure 12. Concentration Profile for Decaying Species – Upper left injection.

(1250 Elements Mesh - Inlet BC: Equation 5; Outlet BC: Equation 10)

Figures 10 and 11 are obtained from the same parameters as those for Figure 9 and in Figure 12 the lateral component of the velocity is set from the upper margin downwards, assuming the negative of Figure 9 case of this same component.

CONCLUSION

In transient reactive flow problems subjected to unsteady BC the main issue is to achieve physical coherence in constructing the model to be solved. Some analytical solutions of this class of problems are found in the literature which, though being parabolic, usually assume the outlet BC in the form of a constant concentration or of a given concentration gradient.

Simulations presented in this work show that oscillatory inlet conditions result in time dependent concentrations at the outlet, not represented by EBCs and NBCs. Also, NBCs may not represent the total equilibrium flux at the outlet (Yu and Singh,

1
2
3
4
5
6
7
8
9
10
11
12
13
14
15
16
17
18
19
20
1995), leading to physically incomplete models that could
21 perform imprecise profile estimation.

22
23
24
25
26
27
28
29
30
31
32
33
34
35
36
37
A new procedure was then proposed, by which a material
38 derivative is considered as the outlet BC. Our results show that
39 these BCs provide a better picture of the process, updating the
40 outlet equilibrium concentration.

41
42
43
44
45
46
47
48
49
50
4 A MATLAB code was developed with a numerical scheme
5 subjected to prescribed stability restrictions (equations 30).
6
7 Good agreement was obtained between simulations and
8 existing analytical solutions, as can be seen on Figures 2 to 4
9 and Table 1. It is also shown in Table 1 and Figure 5
10 comparisons of numerical solutions using EBC, NBC and the
11 proposed MDBC, evidencing the positive aspects of applying
12 the material derivative as the outlet BC. Following, 2-D
13 simulations were then performed in rectangular channels,
14 assuming fully developed velocity profiles.

15
16
17
18
19
20
21
22
23
24
25
26
27
28
29
30
31
32
33
34
35
36
37
38
39
40
41
42
43
44
45
46
47
48
49
50
51
The code features a certain flexibility for automatically
52 generating regular triangular and quadrangular meshes that
53 could be selected to the applicable case. There was also the
54 option of changing the number of GQ points to evaluate the
55 model integrals, known to slightly affect the computational
56 time.

57
58
59
60
Several simulations were run on a i5 CPU notebook, limited
to a maximum of 2000 element meshes, all requiring few
minutes to run, showing that even more refined meshes could

be used while keeping CPU times within acceptable limits. Our tests indicate that the numerical scheme is sufficiently tested to be implemented in codes written in lower level languages.

Finally, a further improvement could be made in the code by future works, in the sense of adopting more elaborated FEM formulations, involving a SUPG or other more advanced stabilization technique, so to combine the advantages of more stable schemes with the proposed adoption of the material derivative as an outlet BC.

NOMENCLATURE

C section-averaged species concentration

C_{appr} approximated concentration given by the FEM formulation

C_{inj} constant injected averaged concentration

$C_{inj}(0,y,t)$ time dependent injected averaged concentration

Da Damköhler Number

D_{x_i} averaged species diffusion coefficient in the direction of coordinate x_i

k reaction constant or pollutant decay constant

L stream length

NN number of nodes in the finite element mesh

Pe Péclet Number

$S_j(x_i)$ shape function

1	\bar{u}_{x_i}	averaged flow velocity along coordinate x_i
2	r	reaction term
3	t	time
4	w	arbitrary weight function
5	x_i	coordinate in an arbitrary direction i
6	Γ	control surface
7	Γ_i	arbitrary boundary
8	Γ_{in}	inlet boundary
9	Γ_{out}	outlet boundary
10	Ω	control volume

ACKNOWLEDGEMENTS

The authors wish to thank the Fundação Carlos Chagas Filho de Amparo à Pesquisa do Estado do Rio de Janeiro (FAPERJ) for its support to this research under the program number E-26/111.079/2013.

REFERENCES

- Aral, M. M. and Liao, B. Analytical Solution for Two-Dimensional Transport Equation with Time-Dependent Dispersion Coefficients., J. Hydrol. Engrg., 1, n°. 1, 20-32 (1996).

1
2
3 Bird, R. B., Stewart, W. E. and Lightfoot, E. N., Transport
4 Phenomena, 2nd ed. John Wiley & Sons, New York (2010).
5
6
7
8
9

10 Chapman, B. M., Dispersion of Soluble Pollutants in Non-
11 uniform Rivers – I. Theory, *J. Hydrol.*, 40, 139-152 (1979).
12
13
14
15

16 Chapra S.C and Canale, R. P., Numerical Methods for
17 Engineers, 6th ed. Mc Graw-Hill, New York (2010).
18
19
20
21
22

23 Czernuszenko, W., Dispersion of Pollutants in Rivers, *Hydr.*
24 *Sci. J.*, 32, n°. 1, 59-67 (1987).
25
26
27
28
29

30 Galante, R. L., Modeling and Simulation of a Continuous
31 Tubular Reactor for the Biodiesel Production (in Portuguese),
32 D.S. Thesis, University of Santa Catarina (2012).
33
34
35
36
37

38 Goltz, W. J. and Dorroh, J. R. The Convection-Diffusion
39 Equation for a Finite Domain with Time Varying Boundaries,
40 Appl. Math. Lett., 14, 983-988 (2001).
41
42
43
44
45
46

47 Kachiashvili, K., Gordezianni, D, Lazarov, R. and
48 Melikdzhanian, D., Modelling and Simulation of Pollutants
49 Transport in Rivers, Appl. Math. Mod., 31, 1371-1396 (2007).
50
51
52
53
54
55
56
57
58
59
60

1
2
3 Launay, M., Le Coz, J., Camenen, B., Walter, C., Angot, H.,
4 Dramais, G., Faure, J.-B. and Coquery, M., Calibrating
5 Pollutant Dispersion in 1-D Hydraulic Models of River
6 Networks, *J. Hydro-env. Res.*, 9, 120-132 (2015).
7
8
9
10
11
12
13

14 Lee, M. E. and Seo, I. W., Analysis of Pollutant Transport in
15 the Han River with Tidal Current Using a 2D Finite Element
16 Model, *J. Hydro-env. Res.*, 1, n°.1, 30-42 (2007).
17
18
19

20
21 Lee, M. E. and Seo, I. W., 2D Finite Element Pollutant
22 Transport Model for Accidental Mass Release in Rivers, *KSCE*
23
24 J. Civ. Eng., 14, n°.1, 77-86 (2010).
25
26
27
28

29
30
31 Levenspiel, O., *Chemical Reaction Engineering*, 3rd ed. John
32 Wiley & Sons, New York (1999).
33
34
35

36
37 Lewis, R. W., Nithiarasu, P. and Seetharamu, K. N.,
38 Fundamentals of the Finite Element Method for Heat and Fluid
39 Flow. John Wiley & Sons, Chichester (2005).
40
41
42
43
44

45
46 Logan, J. D. Solute Transport in Porous Media with Scale-
47 Dependent dispersion and Periodic Boundary Conditions, *J.*
48 *Hydr.*, 184, n°. 3, 261-276 (1996).
49
50
51
52
53
54
55
56
57
58
59
60

1
2
3 Logan, J. D. and Zlotnik, V. The Convection-Diffusion
4
5 Equation with Periodic Boundary Conditions, Appl. Math.
6
7 Lett., 8, n°. 3, 55-61 (1995).
8
9

10
11 Mushtaq, F., Analysis and Validation of Chemical Reactors
12 Performance Models Developed in a Commercial Software
13 Platform, M.S. Thesis, KTH School of Industrial Engineering
14 and Management, Stockholm (2014).
15
16
17
18
19

20
21 O'Loughlin, E. M. and Bowmer, K. H., Dilution and Decay of
22 Aquatic Herbicides in Flowing Channels, J. Hydrol., 26, 217-
23 235 (1975).
24
25
26
27
28

29
30 Ranade, V. V., Computational Flow Modeling for Chemical
31 Reactor Engineering. Academic Press, San Diego (2002).
32
33
34
35
36
37

38 Skrzypacz, P. and Tobiska, L., Finite Element and Matched
39 Asymptotic Expansion Methods for Chemical Reactor Flow
40 Problems, Proc. Appl. Math. Mech., 5, 843-844 (2005).
41
42
43
44
45
46

47 Skrzypacz, P., Finite Element Analysis for Flow in Chemical
48 Reactors, Dr. Rer. Nat. Dissertation, Otto von Guericke
49 Universität, Magdeburg (2010).
50
51
52
53
54
55
56
57
58
59
60

1
2 van der Perk, M., Soil and Water Contamination, 2nd ed.
3
4 CRC/Balkema, Leiden (2013).
5
6
7
8
9
10
11
12
13
14
15
16
17
18
19
20
21
22
23
24
25
26
27
28
29
30
31
32
33
34
35
36
37
38
39
40
41
42
43
44
45
46
47
48
49
50
51
52
53
54
55
56
57
58
59
60

van Genuchten, M. Th. and Alves, W. J. Analytical Solutions
of the One-Dimensional Convective-Dispersive Solute
Transport Equation, US Dept. of Agric. Tech. Bull, no. 1661
(1982).

Vilhena, M.T. and Leal, C. A., Dispersion of Non-Degradable
Pollutants in Rivers, Int. J. Appl. Radiat. Isot., 32, 443-446
(1981).

Vilhena, M.T. and Sefidvash, F., Two-dimensional Treatment
of Dispersion of Pollutants in Rivers, Int. J. Appl. Radiat. Isot.,
36, n°. 7, 569-572 (1985).

Yu, F. X. and Singh, V. P., Improved Finite Element Method
for Solute Transport, J. Hydraul. Eng., 121, n°. 2, 145-158
(1995).

Yu, T.S. and Li, C. W., Instantaneous Discharge of Buoyant
Fluid in Cross-flow, J. Hydraul. Eng., 124, n°. 1, 1161-1176
(1998).

1
2
3 Zienkiewicz, O. C. and Taylor, R. L., The Finite Element
4 Method, Vol 1: The Basis, 5th ed. Butterworth-Heinemann,
5
6 Oxford (2000).
7
8
9
10
11
12
13
14
15
16
17
18
19

20
21 Ziskind, G., Shmueli, H. and Gitis, V., An Analytical Solution
22 of the Convection-Dispersion-Reaction Equation for a Finite
23 Region with a Pulse Boundary Condition, Chem. Eng. J., 167,
24 403-408 (2011).
25
26
27
28
29
30
31
32
33
34
35
36
37
38
39
40
41
42
43
44
45
46
47
48
49
50
51
52
53
54
55
56
57
58
59
60